

Preparation and characterization of conducting copolymer films from 5-aminoquinoline and aniline

H. A. ABD EL-RAHMAN

Chemistry Department, Faculty of Science, Cairo University, Giza, Egypt

Received 21 October 1996; revised 10 December 1996

Conducting copolymer films from 5-aminoquinoline and aniline (abbreviated PAq-An) were prepared by anodic polymerization of different molar ratios of the corresponding monomers in MeCN using cyclic voltammetry and potential step methods. Ellipsometric measurements on the different copolymers indicated that the thickness increases linearly with the anodic charge but with different efficiencies. The electroactivity of the copolymers is attributed to polyaniline in the films and increases as the ratio of aniline in the polymerization solution increases. The copolymer PAq-An(1:5) shows even better electroactivity than polyaniline films prepared under the same conditions due to the higher polymerization efficiency and stability of the former films. Analysis of the spectroelectrochemical measurements in acid solutions showed that the redox peaks of the copolymer PAq-An(1:5) are composed of two consecutive redox processes. Models for the redox processes are proposed to analyse the spectroelectrochemical transient behaviour of the copolymer.

1. Introduction

Due to the electrochemical activity of polyaniline in aqueous acid and nonaqueous solutions, numerous applications, such as rechargeable batteries, electrochromic devices and pH-sensors have been proposed and investigated [1–9]. Since the durability, life cycle and chrono-electrochromic response in solutions are limited, modification of the polymer (e.g., via copolymerization) is advantageous. Anodic polymerization of 5-aminoquinoline was found to yield thin, homogeneous, and stable polymeric films of limited electroactivity [10]. Poly-5-aminoquinoline (PAq) was found to support the attachment of soluble redox species via electrostatic attraction at the quaternary ammonium sites in the polymer. Copolymerization of PAq with a conducting polymer like polyaniline may result in a new attractive polymeric structure which has mixed properties of both polymers. In the present work, oxidative polymerization of different ratios of aniline and 5-aminoquinoline in MeCN and characterization of the resulting films in aqueous acid and non-aqueous solutions are studied. Since the electroactivity of the copolymer PAq-An(1:5) was found to be even higher than that of polyaniline films prepared under the same conditions, the spectroelectrochemical and microgravimetric studies are concentrated on that copolymer.

2. Experimental details

5-aminoquinoline (Aldrich, 97%), aniline and tetrabutyl ammonium perchlorate, TBAP, (Fluka, Germany, AR grade) were used without further purification. MeCN (Janssen, Germany, AR grade)

was doubly distilled. The aqueous solutions were prepared from analytical grade chemicals and de-ionized 'millipore' water. The working electrodes were either gold wires with a diameter of 400 nm or gold films evaporated on glass; 200 nm Au/10 nm Ti/glass (area 0.90 cm²). The counter electrode was a gold sheet (area 2.0 cm²). The reference electrodes were Hg/Hg₂Cl₂/0.1 M tetrabutyl ammonium chloride (MeCN); $U = -0.023$ V, vs SHE, in MeCN, and a Hg/Hg₂(SO₄)₂/0.5 M H₂SO₄; $U = 0.680$ V, in sulfuric acid solutions. An integrated home-built potentiostat with a fast autoranging amplifier and a positive feed-back IR-compensation was used for cyclic voltammetry and potential-step measurements. Ellipsometric measurements were carried out on polymer samples prepared on electrodes of 200 nm Au/10 nm Ti/glass by cyclic voltammetry using an automatic ellipsometer (AFE 401, Sentech., Germany) with He-Ne laser of $\lambda = 632.8$ nm and $P = 5$ mW. For the quartz crystal microbalance measurements, 5 MHz AT-cut 13 mm diameter quartz crystals, with sputtered circular 150 nm thick gold electrodes on both sides of the crystals (geometric area of each electrode 0.283 cm²) were positioned in special holders to allow the contact of both electrodes to the resonance circuit and the frequency counter and only one electrode surface with the electrolyte. The mass sensitivity was determined by copper deposition and found to be 18 ng Hz⁻¹ cm⁻². UV and vis. spectroscopy was carried out on samples prepared on ITO glass electrodes (surface resistance $\sim 10 \Omega$ cm⁻²) using a full computerized spectroscopic system (OMS-4, EP&S Karger Elektronik, Lin/Rhein) capable of recording up to 500 spectra (range 180–1100 nm) in a minimum time of 16 ms per

spectrum through 1024 pixels. All electrochemical experiments were carried out at a temperature of 20 °C under nitrogen.

3. Results and discussion

3.1. Formation of the copolymers

Different copolymers were prepared by cyclic voltammetry and potential step methods on gold electrodes in MeCN containing 0.1 M TBAP and different molar ratios of 5-aminoquinoline : aniline; namely, 10 mM 5-aminoquinoline + 2 mM aniline; PAq-An(5:1), 10 mM 5-aminoquinoline + 5 mM aniline; PAq-An(2:1), 10 mM 5-aminoquinoline + 10 mM aniline; PAq-An) 1:1, and 1 mM 5-aminoquinoline + 5 mM aniline or 4 mM 5-aminoquinoline + 20 mM aniline; PAq-An(1:5). The ratios given between parentheses refer to the monomer ratios in the polymerization solution and the ratios in the copolymers may not be the same. Cyclic voltammograms for the copolymerization of one of these mixtures is shown in Fig 1. The main oxidation peak at 1.24 V vs SHE is attributed to the oxidation of the primary aromatic amines [11]. Generally, the main oxidation peak shifts to higher potentials and the peak currents increase as the aniline ratio increases. The next oxidation peak at ~ 2 V is due to the oxidation of the quinoline ring [12]. The redox peaks at ~ 0.5 V are due to the electroactivity of the growing polymer films and increase as the number of scan or aniline ratio increases. The polymerization process is accompanied by intensive oligomer formation, especially at the beginning. The film colour and morphology depends on the copolymer type and formation charge. Generally, the colours of copolymers are intermediate between those of PAq (yellow-brown) and PAn (faint green in reduced state-bluish green in the oxidized state).

The response of the quartz crystal microbalance (QCM) during the cyclovoltammetric deposition of

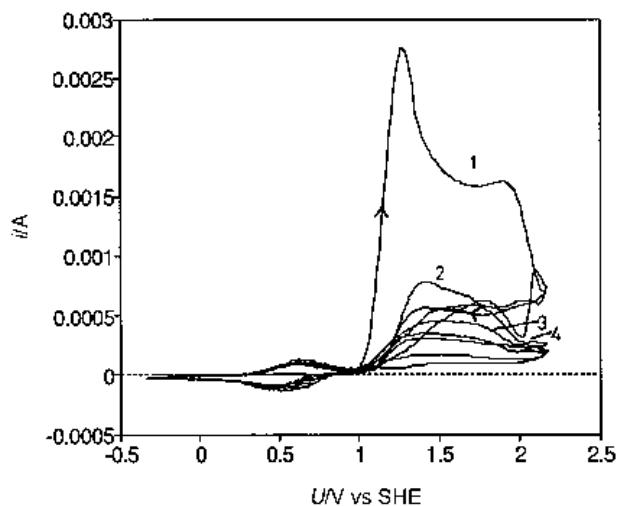


Fig. 1. Cyclic voltammograms for the oxidative polymerization of 4 mM 5-aminoquinoline and 20 mM aniline in MeCN containing 0.1 M TBAP. Numbers refer to the number of cycle. Electrode area 0.22 cm².

PAq-An (1:5), Fig. 2(a), shows that the resonating frequency decreases (i.e. mass increase) with increasing number of cycles due to the deposition of adherent and compact (rigid) polymeric films. As can be seen in Fig. 2(b), the mass gain does not change linearly with the formation charge but it increases significantly as the number of cycles increases. This is due to increasing the ratio of polymer/oligomer. Due to the autocatalytic nature of the oxidative polymerization of aniline, the depositing polyaniline ratio increases as the number of cycles increases.

Since the polymerization solutions are coloured and intensive soluble oxidation products change the solution composition, *in situ* ellipsometry was not feasible. Thus, *ex situ* ellipsometric study on thin copolymer films was carried out to estimate the optical parameters, namely the refractive index of the polymer film, n_1 , and its extinction coefficient, k_1 , and thickness. The films were prepared by different numbers of cycles from 0 to 1.6 V at 50 mV s⁻¹ and removed from solution after holding the potential at 0.8 V for 2 min (i.e., the films were in the oxidized state). At first, two films of different thicknesses were independently used to determine n_1 and k_1 by using the procedure of the angle of incidence variation at five angles (44°–75°) [10, 13]. The refractive index and extinction coefficient of the Au substrate, n_2 and k_2 , were found to be 3.10 and 0.20, respectively. A special

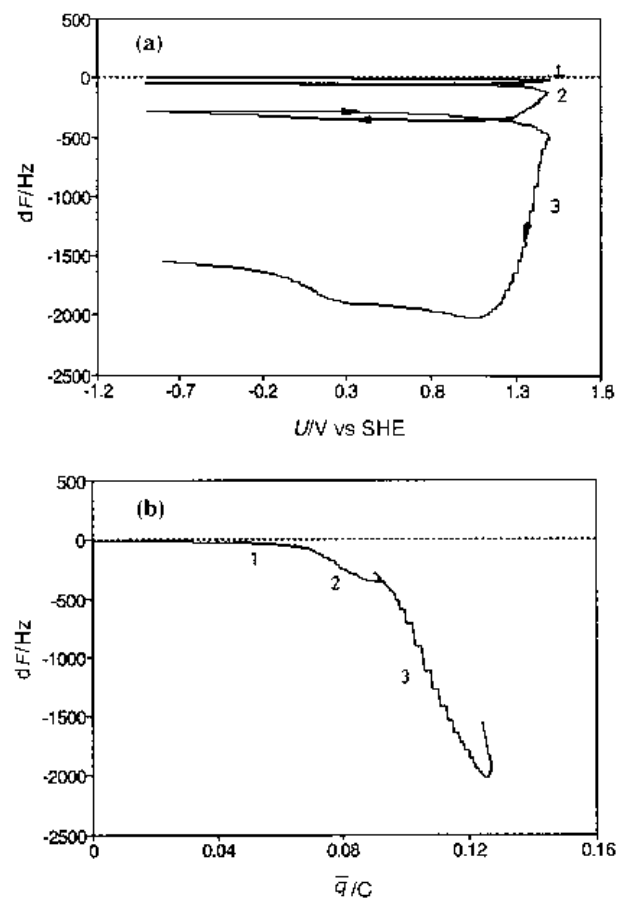


Fig. 2. Decrease in frequency, dF , with potential (a) and charge (b) during the oxidative polymerization of 4 mM 5-aminoquinoline and 20 mM aniline in MeCN containing 0.1 M TBAP. Electrode area 0.283 cm².

home-written fitting program was used to fit the automatically measured ellipsometric angles; Δ and Ψ , into a one layer model [13, 14]. Generally, the optical parameters of the two samples were the same. Consequently, the thicknesses of the rest of each copolymer were determined by direct measurement using the ellipsometer software. The optical parameters of the different copolymers are given in Table 1. The dependence of the film thickness on the formation charge, \bar{q} , for different copolymers and PAq is shown in Fig. 3(a). The thickness increases practically linearly with the amount of charge passed. The results indicate substantial differences in the copolymer characteristics, for example, the polymerization efficiency, density etc. Extrapolation of $d-\bar{q}$ curves to $d = 0$ give the charge, \bar{q}_0 , which is consumed in soluble oxidation products at the beginning of the polymerization process and deposition of the polymer film. Figure 3(b) shows that the growth of the copolymer PAq-An(1:5) is more efficient at lower concentrations, although it requires more formation cycles.

3.2. Electroactivities of the copolymers

The electroactivities of the copolymer films on gold electrodes were tested in MeCN and aqueous H_2SO_4 acid solutions. Since the electroactivity of PAq has previously been found to be negligible [10], the electroactivities of the copolymers are expected to be due to polyaniline in films or a new structure for the copolymer. The fact that the electroactivities (redox peaks) of the copolymers are similar to those of polyaniline excludes the latter assumption. Figure 4 shows the electroactivities of some copolymers in comparison with PAn films formed by the same procedure (five cyclovoltammetric scans) in MeCN. The charge involved in the formation of PAn and the copolymers PAq-An(1:5), PAq-An(1:1) and PAq-An(2:1) were 0.62, 0.47, 0.32 and 0.11 C cm^{-2} , respectively. The redox charge depends strongly on the

Table 1. The optical parameters, n_1 , k_1 , used to estimate the ex situ thickness for films of different copolymers

Copolymer	Polymerization solution	n_1	k_1
PAq	10 mM 5-aminoquinoline + 0.1 M TBAP (MeCN)	1.26	0.040
PAq-An(2:1)	10 mM 5-aminoquinoline + 5 mM aniline + 0.1 M TBAP (MeCN)	1.32	0.098
PAq-An(1:1)	10 mM 5-aminoquinoline + 10 mM aniline + 0.1 M TBAP (MeCN)	1.50	0.130
PAq-An(1:5)	1 mM 5-aminoquinoline + 5 mM aniline + 0.1 M TBAP (MeCN)	1.25	0.037
PAq-An(1:5)	4 mM 5-aminoquinoline + 20 mM aniline + 0.1 M TBAP (MeCN)	1.11	0.083

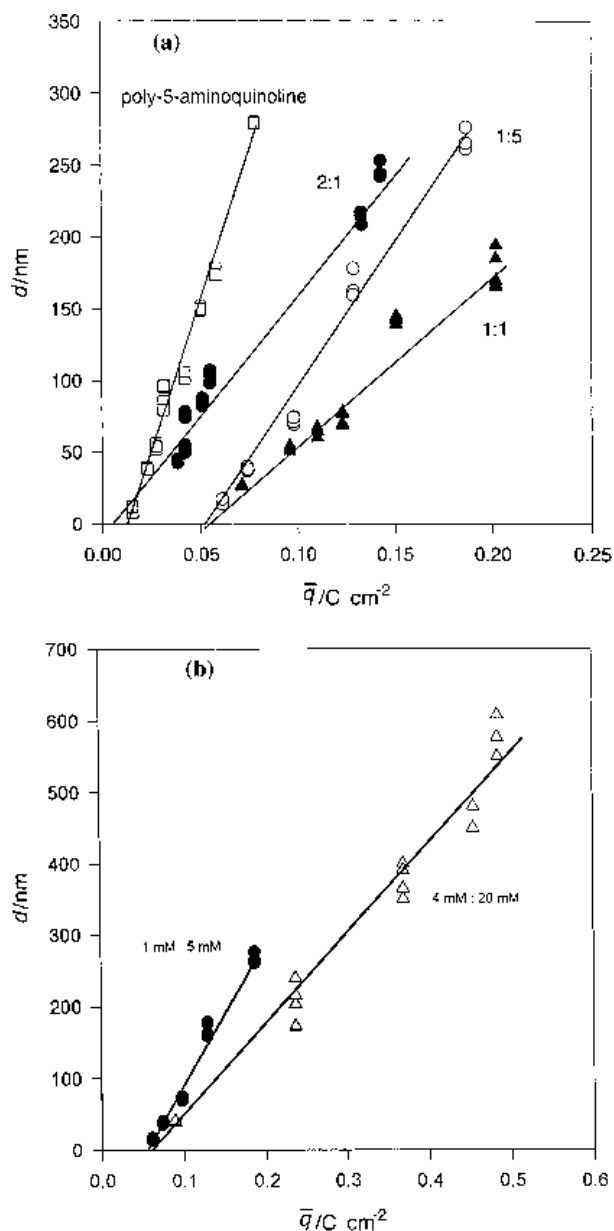


Fig. 3. (a) Film thickness, d against charge of formation, \bar{q} , for different copolymers and poly-5-aminoquinoline; (\square) PAq, (\bullet) PAq-An(2:1), (\blacktriangle) PAq-An(1:1) and (\circ) PAq-An(1:5). The optical parameters used are given in Table 1. (b) Film thickness of PAq-An(1:5) formed by two different monomer concentrations; (\bullet) 1 mM 5-aminoquinoline : 5 mM aniline and (\triangle) 4 mM 5-aminoquinoline : 20 mM aniline.

aniline amount in the copolymer. The copolymer PAq-An(1:5) has a higher redox charge than poly-aniline, although its formation charge is less. This behaviour is not surprising, since the actual amount of the deposited polymeric material is higher for PAq-An(1:5) due to the stabilizing effect of PAq (i.e., less oligomer formation).

In the rest of the measurements films of PAq-An(1:5) deposited from 4 mM 5-aminoquinoline + 20 mM aniline were employed due to their superior properties. QCM response for the electroactivity of PAq-An(1:5) in MeCN shows a continuous decrease in the resonating frequency (i.e., mass loss from the rigid polymeric layer on the balance surface) during the anodic scan and the reverse trend in the

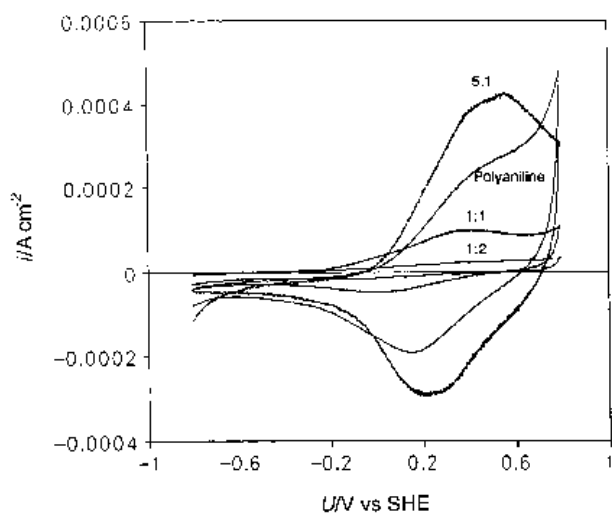


Fig. 4. Electrochemical activity of different copolymers of PAq-An and PAN in MeCN containing 0.1M TBAP. Scan rate 50 mV s^{-1} . The ratios given refer to the ratios of monomers (5-aminoquinoline:aniline) in the polymerization solution.

cathodic scan with a pronounced hysteresis, Fig. 5. The behaviour indicates the insertion of species on oxidation of the copolymer and removal of species on reduction [15, 16]. Since the oxidation involves charging of the film positively, anions are expected to move into the film to neutralize the excess charge and

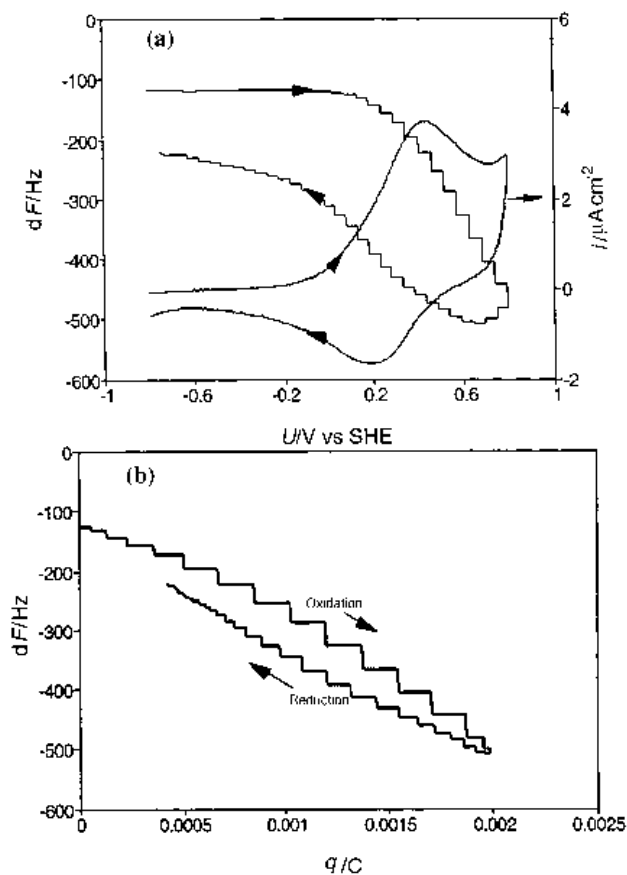


Fig. 5. (a) Cyclic voltammogram and change in frequency, dF , for PAq-An(1:5) in 0.1M TBAP (MeCN), Scan rate 20 mV s^{-1} . The films were formed by three cycles from 0 to 1.6V at 50 mV s^{-1} ; $\bar{q} = 126 \text{ mC cm}^{-2}$. (b) Change in frequency, dF , as a function of the redox charge. Electrode area 0.283 cm^2 .

to exit on reduction. The hysteresis indicates that the insertion/removal process is not reversible (fast). This is because either the rate of insertion of species is higher than their removal or both are slow within the used scan rate of 20 mV s^{-1} . The mass change is approximately a linear function of the redox charge, Fig. 5, with a slope proportional to the molecular mass of the inserted/removed species ($\sim 98 \pm 1 \text{ g mol}^{-1}$). This value corresponds to the insertion/removal of one ClO_4^- (99.5 g mol^{-1}). The copolymers are also electroactive in aqueous H_2SO_4 acid solutions due to an electron + proton elimination/addition process at the imino groups like PAN [3, 5] as can be seen in Fig. 6. The role of PAq in films manifests itself on the redox peaks in two ways. First, the anodic and cathodic peaks are symmetrical, in contrast to the known asymmetric peaks for PAN. Second, the peak potential (and peak separation) was found to increase linearly with the square root of scan rate, as usually observed for processes controlled by film resistance [24]. As can be seen in Fig. 7, the peak currents vary according to the expected behaviour for strongly at-

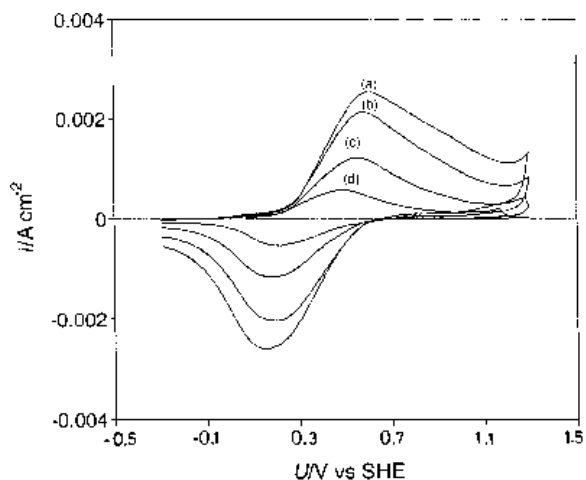


Fig. 6. Effect of scan rate on cyclic voltammograms for PAq-An(1:5) in 0.5M sulfuric acid. (a) 150, (b) 100, (c) 50 and (d) 20 mV s^{-1} . The films were formed by 10 cycles from 0 to 1.8V; $\bar{q} = 452 \text{ mC cm}^{-2}$.

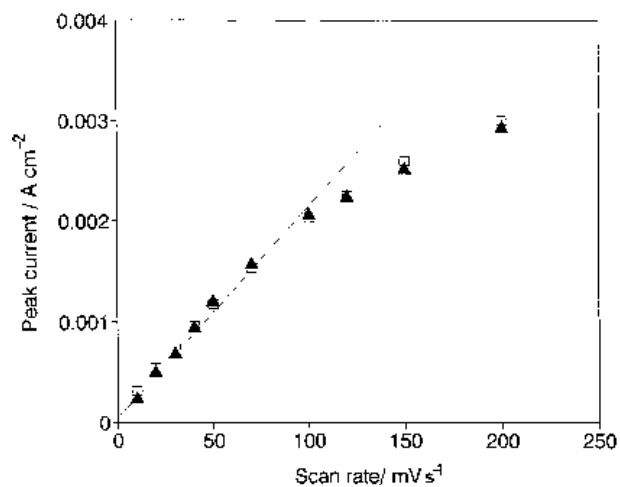


Fig. 7. The peak current against scan rate for PAq-An(1:5). Key: (▲) anodic and (□) cathodic.

tached electroactive species (peak current vs. scan rate is linear up to $\sim 100 \text{ mV s}^{-1}$) followed by a semi-infinite linear diffusion at higher scan rates (peak current vs. square root of scan rate $> 100 \text{ mV s}^{-1}$ is linear) [11].

3.3. Spectroelectrochemistry of the copolymer(1:5)

3.3.1. Nernstian behaviour. Ultraviolet and visible spectra for films of PAq-An(1:5) on ITO electrodes in $0.5 \text{ M H}_2\text{SO}_4$ were monitored as a function of potential in the potential range from the fully reduced form to the fully oxidized form. It should be mentioned that the anodic charge passed (and consequently the amount of the deposited copolymer) during the oxidative polymerization by using ITO electrodes are substantially lower than that passed when gold electrodes were used under the same conditions of the final potential and number of cycles. The absorption spectra of PAq-An(1:5) are similar to those of PAn, though the bands are broader, Fig. 8 [17, 18]. Although the highest absorption occurs at a wavelength of $\sim 330 \text{ nm}$, the highest difference in the absorptivity between the redox forms of PAq-An(1:5) occurs in the red region at $\sim 570 \text{ nm}$. The absorption at a higher wavelength $> 500 \text{ nm}$ is mainly due to the oxidized form while that at $\sim 330 \text{ nm}$ includes contributions of both the reduced and the oxidized forms, but it decreases slightly as the ratio of the oxidized form increases [17, 18]. The absorption peak at $\sim 430 \text{ nm}$ (relatively higher for PAn) shows an absorbance maximum at a certain potential (or redox ratio) and is attributed to the partially oxidized form. The not well-defined isosbestic points at about 370 and 460 nm indicate two quasi-equilibria that involve neutral copolymer/polaron and polaron/bipolaron, respectively [18–20]. Using the absorbances at 329 and 570 nm , the $[\text{ox}]/[\text{red}]$ ratios were calculated, respectively, from the relations [9]:

$$[\text{ox}]/[\text{red}] = A(-0.2 \text{ V}) - A(U) / A(U) - A(0.9 \text{ V}) \quad (1)$$

$$[\text{ox}]/[\text{red}] = A(U) - A(-0.2 \text{ V}) / A(0.9 \text{ V}) - A(U) \quad (2)$$

where $A(-0.2 \text{ V})$ and $A(0.9 \text{ V})$ are the absorbances for the fully reduced and fully oxidized forms, re-

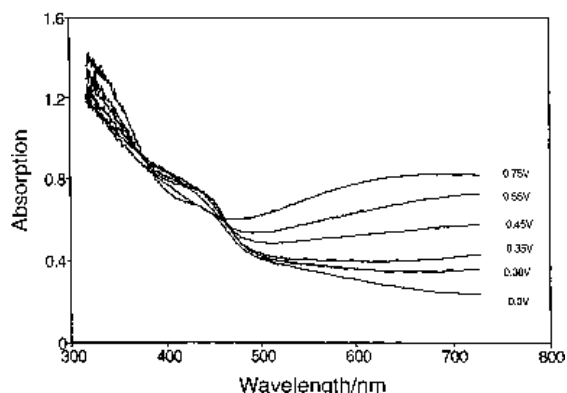


Fig. 8. Absorption spectra for PAq-An(1:5) in $0.5 \text{ M H}_2\text{SO}_4$ at different potentials. The films were formed on ITO electrodes by cyclic voltammetry from 0 to 1.8 V ; $\bar{q} = 70 \text{ mC cm}^{-2}$.

spectively, and $A(U)$ is the absorbance at potential U . The above relations assume the application of Beer's law. Strictly speaking, A is related to the surface concentration, $\Gamma_{\text{ox}}/\Gamma_{\text{red}}$, not the concentration itself, $[\text{ox}]/[\text{red}] = (\Gamma_{\text{ox}}/\Gamma_{\text{red}})(d_{\text{ox}}/d_{\text{red}})$, and some knowledge of thickness is necessary. An *in situ* ellipsometric study showed that thickness of PAn increases with potential in the same manner as the redox charge (i.e., the surface concentration) [25]. Thus, the absorbencies can still be used as a first approximation, but a higher slope for the Nernst relation is expected. Figure 9 shows Nernstian behaviour of PAq-An(1:5) using the concentration ratios given by relations 1 and 2. As can be seen, linearity holds over more than two orders of magnitude of concentration ratio for each of the two redox processes. For the redox processes of neutral/polaron and polaron/bipolaron (appearing in cyclic voltammetry as one pair of redox peaks), the formal redox potentials are 0.268 and 0.447 V and Nernst slopes are 0.210 and $0.260 \text{ V decade}^{-1}$, respectively. The theoretical slopes for the redox processes mentioned above should be $0.06 \text{ V decade}^{-1}$ at 30°C , when one electron per

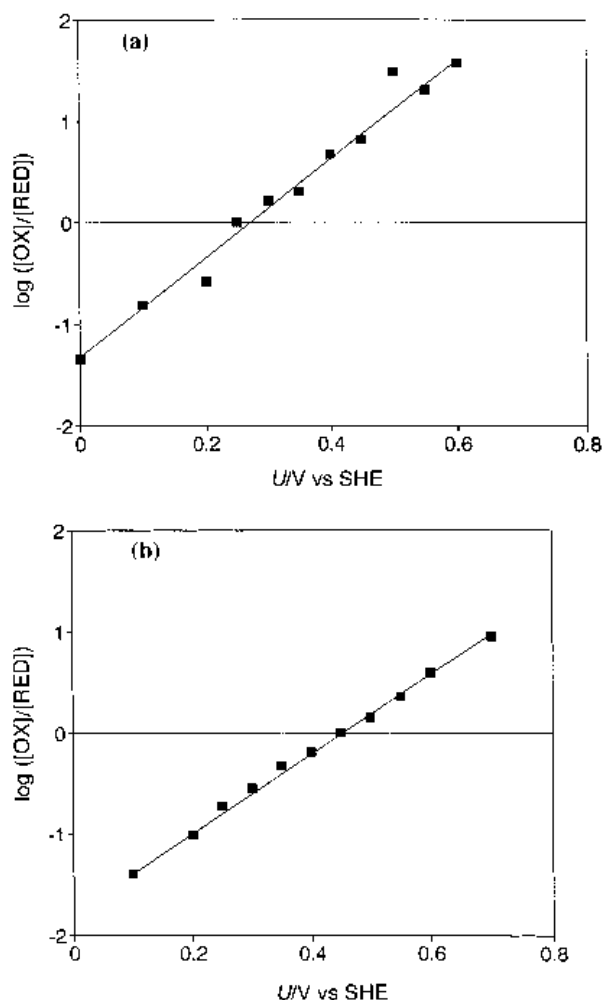


Fig. 9. Nernst relation for PAq-An(1:5) in $0.5 \text{ M H}_2\text{SO}_4$ at $\lambda = 329 \text{ nm}$ (a) and 570 nm (b). Details as for Fig. 8. For (a): slope $210 \text{ mV decade}^{-1}$ and $[\text{ox}]/[\text{red}] = A(-0.2 \text{ V}) - A(U) / A(U) - A(0.9 \text{ V})$; for (b): slope $260 \text{ mV decade}^{-1}$ and $[\text{ox}]/[\text{red}] = A(U) - A(-0.2 \text{ V}) / A(-0.9 \text{ V}) - A(U)$.

monomer unit is considered. High slopes were also reported for the redox processes of polypyrrole [19] and the deviation was interpreted in terms of excess chemical potential which originates from the fact that the unit cell in polaron and bipolaron consists of several monomers. This means that the concentration of redox species contributing to the Nernst equation are underestimated as compared to a unit cell of one monomer and the apparent number of electrons becomes fractional (i.e., slopes > 0.06 V decade $^{-1}$).

3.3.2. Transient behaviour. The change in absorption spectra with time after stepping the potential from -0.2 to 0.9 V for PAq-An(1:5) in 0.5 M H_2SO_4 solutions is shown in Fig. 10. The main change occurs in the region of the oxidized form absorption, where the absorbance increases as the oxidation time increases until the copolymer film is completely oxidized. The reduction showed the opposite trend. The absorbance of the fully oxidized form at 570 nm was selected to monitor the transient behaviour of the redox processes. The time-dependence of absorbance for the two processes are different and may be explained for a first approximation by simple models. To support the models introduced to explain the spectroscopic measurements, the corresponding chronocoulometric responses were also recorded under the same conditions. For homogenous electroactive film, the absorbance, $A(\lambda_{max})$ of the oxidized/reduced form is related to the charge, q , consumed in its reduction/oxidation via the relation [17]:

$$A = \epsilon q / nF \quad (3)$$

where ϵ is molar absorptivity. Under ideal conditions, Relation 3 serves as a quantitative correlation between molecular absorption spectroscopy and electrochemistry.

(a) High field model for the oxidation process

For polymer films which involve substantial change in the electronic properties on electrochemical

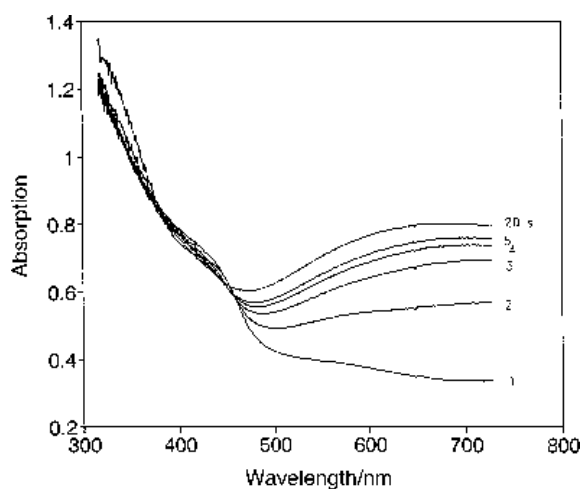


Fig. 10. Absorption spectra for PAq-An (1:5) at different times in seconds after switching the potential from 0.0 to 0.8 V. The films were formed on ITO electrodes by cyclic voltammetry; $\bar{q} = 85$ mC cm $^{-2}$.

switching from the reduced (insulating) form to the oxidized (conducting) form, it is assumed that the oxidation, under potentiostatic control, starts at the electrode/polymer interface due to the insulating properties of the films in the reduced form [22] and is controlled by the charge and ion transfer through the reduced part of the film. The total potential drop across the metal/electrolyte interface is

$$U = U_{red} + U_{ox} + U_{el} + U_{mp} \sim U_{red} + U' \quad (4)$$

where U_{red} , U_{ox} , U_{el} and U_{mp} are, respectively, the potential drops cross the reduced and oxidized layers, and the interfaces of polymer/electrolyte and metal/polymer. Since the conductivity of the oxidized form \gg reduced form, $U_{ox} \ll U_{red}$ and it is further assumed that U_{el} and U_{mp} are constant during the reduction process, that is, U' is a constant. The rate of the ionic transfer, R , is assumed to obey the high field law which usually holds during formation of insulating oxide films [23]:

$$R = dx_{red}/dt = k \exp(BH_{red}) \quad (5)$$

where H_{red} is the field strength across the reduced layer and k and B are constants and R is given in terms of increasing layer thickness, x_{red} . After integrating Relation 5, the following relation is obtained:

$$(1/k) [x_{red}^2/B(U - U')] \exp[-B(U - U')/x_{red}] = t \quad (6)$$

Taking the logarithms of both sides of Relation 4 and appropriate rearrangement yields:

$$[B(U - U')/x_{red}] - \ln [x_{red}^2/B(U - U')] = -\ln t + C \quad (7)$$

where C is a constant. Using the absorbance of the oxidized form, x_{red} is given by

$$x_{red} = (x_{ox,o}/A_o) (A_o - A) \quad (8)$$

where the subscript 'o' refers to the fully oxidized form. Substitution of x_{red} from Equation 8 in Equation 7 and rearrangement gives:

$$1/(A_o - A) = B' [\log(A_o - A)/t] + C' \quad (9)$$

where B' and C' are constants. The application of Relation 9 in the case of oxidation of PAq-An(1:5) is shown in Fig. 11. According to Relation 3, replacement of the absorbance by the charge should show the same behaviour, Fig. 12. The dashed line in Fig. 12 refers to the time period covered by spectroscopic data in Fig. 11 and in that time period 80% of the anodic charge was consumed.

(b) Reduction process

Due to the high conductivity of the oxidized form, the reduction process, after a small reduction charge, proceeds through the conducting channels in the film. Both mass and charge transfer are rapidly impeded and the following rate of reduction is assumed:

$$-dC_{ox}/dt = k \exp[aC_{ox}] \quad (10)$$

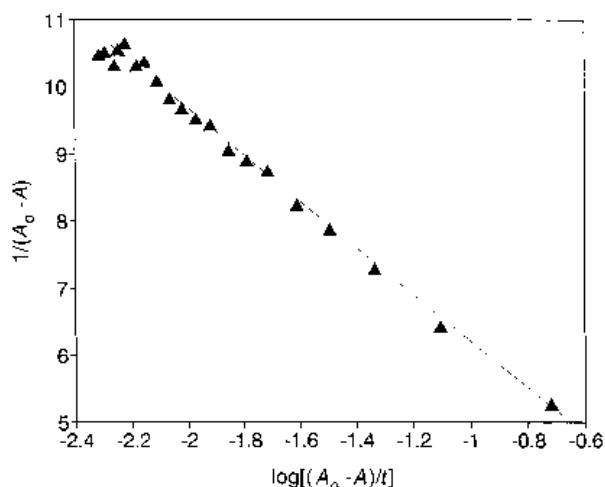


Fig. 11. Transient behaviour of absorbance (A) according to the proposed model (Equation 9) for the oxidation process of PAQ-An(1:5) in 0.5M H_2SO_4 .

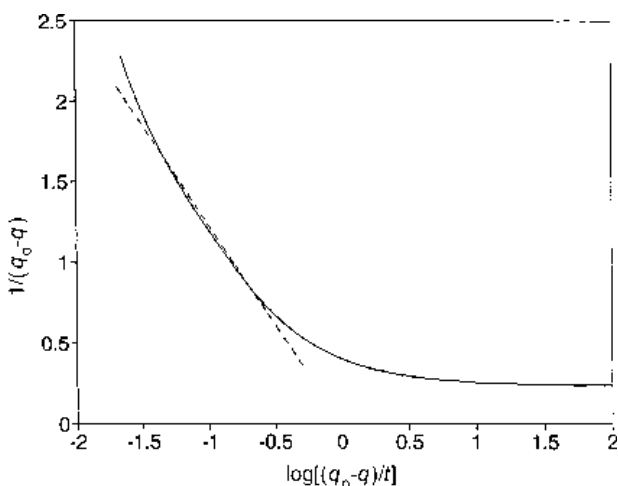


Fig. 12. Transient behaviour of charge (q) according to the proposed model (Equation 3 and 9) for the oxidation process of PAQ-An(1:5) in 0.5M H_2SO_4 . The dashed line refers to the time scale covered by spectroscopic data in Fig. 11.

Integration of Equation 10 and rearrangement, gives

$$C_{ox} = -\log(t + m) + m' \quad (11)$$

where m and m' are constants. Using the absorbance of the oxidized form, Equation 11 becomes

$$A = -P \log(t + m) + m'' \quad (12)$$

where P and m'' are constants. Application of Relation 12 for the reduction of PAQ-An(1:5) is shown in Fig. 13. Replacement of the absorbance by the charge shows the same behaviour as can be seen in Fig. 14. The dashed line in the figure corresponds to the time period covered by spectroscopic data in Fig. 13 and indicates that $\sim 85\%$ of the cathodic charge could be explained according to the proposed model and Equation 12.

4. Conclusion

Conducting copolymers from 5-aminoquinoline and aniline were formed by oxidative polymerization in

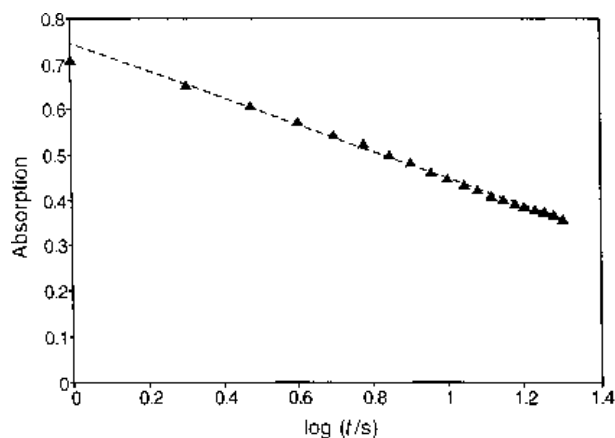


Fig. 13. Transient behaviour of absorbance (A) according to the proposed model (Equation 12) for the reduction process of PAQ-An(1:5) in 0.5M H_2SO_4 .

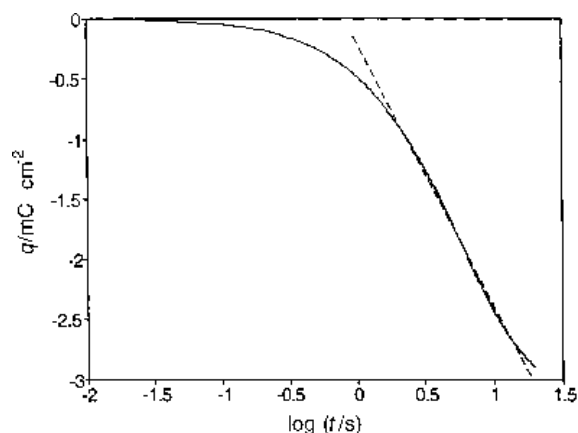


Fig. 14. Transient behaviour of charge (q) according to the proposed model (Equation 3 and 12) for the reduction process of PAQ-An(1:5) in 0.5M H_2SO_4 . The dashed line refers to the time scale covered by spectroscopic data in Fig. 13.

MeCN and showed electroactivity due to polyaniline in films. Due to the presence of poly-5-aminoquinoline, however, several properties of PAQ-An(1:5) were modified (e.g., the redox charge increased) the redox peaks became symmetrical and a Nernstian behaviour of the two redox processes involved was confirmed. Analysis of the transients for the redox processes showed that the oxidation proceeds according to a high field law while in the reduction the concentration of the oxidized sites decreases exponentially with time.

Acknowledgements

The author is thankful to Professor Dr. J.W. Schultze at Dusseldorf University for his support and helpful discussion and Alexander von Humboldt foundation for financial support.

References

- [1] A. R. Hillman, 'Electrochemical Science and Technology of Polymers' (edited by R. G. Linford), Elsevier Applied Science, London(1987).

- [2] T. Ohsaka, Y. Ohnuki, N. Oyama, G. Katagiri and K. Kamisaka, *J. Electroanal. Chem.* **161** (1984) 399.
- [3] T. Kobayashi, H. Yoneyama and H. Tamura, *ibid.* **161** (1984) 419; *ibid.* **177** (1984) 281, 293.
- [4] A. Kitani, J. Yano and K. Sasaki, *J. Electroanal. Chem.* **209** (1986) 227.
- [5] E. M. Genies and C. Tsintavis, *ibid.* **195** (1985) 109; *ibid.* **220** (1987) 67.
- [6] S. Kuwabata, K. Mitsui and H. Yoneyama, *ibid.* **281** (1990) 97.
- [7] E. M. Genies, J. F. Penneau and E. Vieil, *ibid.* **283** (1990) 205.
- [8] T. Sawai, H. Shinohara, Y. Ikariyama and M. Aizawa, *Anal. Chem.* **283** (1990) 221.
- [9] T. Ohsaka, S. Ogano, K. Naoi and N. Oyama, *J. Electrochem. Soc.* **283** (1990) 221.
- [10] H. A. Abd El-Rahman and J. W. Schultze, *J. Electroanal. Chem.*, in press.
- [11] A. Volkov, G. Tourillon, P. Lacaze and J. Dubois, *ibid.*, **115** (1980) 279.
- [12] G. Jones, 'Quinolines', Part I, Wiley, London, (1977) p. 5 and p. 599.
- [13] S. Kudelka, A. Michaelis and J. W. Schultze, *Ber. Bunsenges. Phys. Chem.* **9** (1995) 1020.
- [14] R. M. A. Azzam and N. M. Bashara, 'Ellipsometry and Polarized Light', North Holland (1977), chapter 4, p. 319.
- [15] A. R. Hillman, M. J. Swann and S. Bruckenstein, *J. Electroanal. Chem.* **291** (1990) 147.
- [16] M. C. Miras, C. Barbero, R. Kotz, O. Haas and V. M. Schmidt, *ibid.* **338** (1992) 279.
- [17] R. Kessel and J. W. Schultze, *Surf. Interface Anal.* **16** (1990) 401.
- [18] K. G. Neoh, E. T. Kang and K. L. Tan, *J. Phys. Chem.* **96** (1992) 6777.
- [19] T. Amemiya, K. Hashimoto and A. Fujishima, *J. Electrochem. Soc.* **138** (1991) 2845.
- [20] J. Ochmanska and P. G. Pickup, *J. Electroanal. Chem.* **271** (1989) 83.
- [21] B. P. Jelle, G. Hagen, S. M. Hesjevik and R. Odegard, *Electrochim. Acta* **38** (1993) 1647.
- [22] O. Genz, M. M. Lohrengel and J. W. Schultze, *ibid.* **39** (1994) 179.
- [23] A. G. Gad-Allah, H. A. Abd El-Rahman and M. M. Abou-Romia, *Br. Corros. J.* **23** (1988) 181.
- [24] A. J. Calandra, N. R. DeTacconi, R. P. Pereiro and A. J. Arvia, *Electrochim. Acta* **19** (1974) 901.
- [25] C. Barbero and R. Kotz, *J. Electrochem. Soc.* **141** (1994) 859.